Chapter 3

Studies on A549 human lung cancer cell line and HET-CAM test revealed that 4-Fluorophenylacetamide-acetyl coumarin hinders metastasis and angiogenesis

The unrestricted growth of the genetically transformed cell leads to a primary heterogeneous mass of cells known as a tumor, and the stage is considered as 'pre-cancerous neoplasm,' which can be cured easily by surgical excisions. However, when these primary tumor cells get transformed due to environmental, genetic, or epigenetic stimulations, they attain the characteristic of metastatic tumors, which can invade the surrounding tissue and colonize in the distant organ of the body. Now they are called a secondary tumor, and the process is known as metastasis. About 90% of cancer-related death is due to the metastasis of the tumor cells rather than the primary tumor itself (Hanahan and Weinberg, 2000). An understanding of tumor cell invasion and metastasis process can be of great help in the breaking of this cascade of events and, subsequently, in the eradication of metastatic cancer. Metastatic tumors either invade neighboring and surrounding tissue directly or disseminate to the distant organ via the circulatory/lymphatic route. It is a multistep process that encompasses, separation from the primary tumor, invasion through primary tissue and ECM degradation, angiogenesis to enter into the circulation, survival, extravasation, and secondary tumor formation.

Here in this chapter, we focused on the initial steps of the metastasis process, includes separation, invasion, and angiogenesis. These are the most critical steps for the metastasis progression, and the genes involve in these processes are known as "metastasis initiation genes" and promote motility, epithelial-mesenchymal transformation (EMT), extracellular matrix degradation and angiogenesis (Chiang and Massagu, 2008). The molecular mediators of the initiation of metastasis include Twist1, Snai1, and Snai2 (also known as Slug), a transcription factor which aberrantly regulated the process of EMT, matrix metalloproteinases (MMPs) - which are needed for the extracellular matrix degradation, VEGFs for angiogenesis, and cytokines which help all these processes.

Initiation of EMT entails the loss of cell-cell adhesion, activation of transcription factors, a shift in the epithelial characteristic, and change in gene expression pattern to acquisite a characteristic mesenchymal, migratory phenotype (Thiery, 2003; Thiery et al., 2009). EMT is a very conserved process that occurs during embryogenesis, chronic inflammation as well as cancer and referred to as type I, II, and III, respectively. It denotes a malignant progression to aggressive carcinoma. One hallmark of EMT is the downregulation or even loss of epithelial (E) cadherin, which is an essential component of adherence junctions (Cavallaro and Christofori, 2004). Essentially, it marked as a process in which epithelial cells lose their polarity and ability to adhere, instead, they gain properties to move, migrate through the extracellular matrix, and become invasive (Oral et al., 2016). E-cadherin is required for the cell-cell contact and binds to an E-cadherin molecule of the neighboring epithelial cell and stabilizes the cell-to-cell contacts. Intracellularly, E-cadherin binds to β-catenin and other catenins, which act as intracellular signaling molecules. Downregulation of E-cadherin by the transcriptional repressors Snail/SNAI1, Slug/SNAIL2, SIP1/ZEB2, or Twist leads to the disassembly of adherence junctions and help the cell to gain mesenchymal characteristic by upregulating the mesenchymal markers such as vimentin and neuronal (N) cadherin a biomarker for the mesenchymal cells (Lehembre et al., 2008, Yilmaz and Christofori, 2010). Downregulation of E-cadherin also leads to translocation of membrane-bound β-catenin to the cell nucleus where it modulates transcription of numerous genes such as c-myc and cyclin D1 (Peinado et al., 2007; Thiery et al., 2009). The subsequent change from E to N-cadherin expression termed cadherin-switch, and help in EMT-transformed cell's motility (Christofori, 2006). Thus, cells that have undergone an epithelial to mesenchymal transformation gain the ability to detach from the tumor cluster in order to move as single cells in a mesenchymal fashion. Another factor that helps the cell in attaining the characteristic of the mesenchymal cell is transforming growth factor-β (TGF- β) which play a central role in tumor progression (Zavadil and Bottinger, 2005, Grusch et al., 2010), by upregulating the transcriptional repressors of E-cadherin (Massague and Wotton, 2000, Thiery, 2002). There are many reports that, in patients with non-small cell lung cancer (NSCLC), undetectable E-cadherin expression minimizes the overall survival rate (Nakashima et al., 2003, Wu et al., 2012). Therefore, the gene regulating the process of epithelial to mesenchymal transformation can be a good target for the NSCLC treatment.

Once tumor cell gets transformed and attained the characteristic of a mesenchymal cell, they start secreting the proteinases to degrade the basement membrane for the active translocation of neoplastic cells across ECM (Woodhouse et al., 1997, Engers and Gabbert, 2000, Mareel and

Leroy, 2003). Matrix metalloproteinases are a family of zinc-dependent endoproteinases whose enzymatic activity results in degradation of the extracellular matrix (ECM). It is known that all invasive malignant tumors, including lung cancer cell lines, express high levels of MMPs. They facilitate tumor cell invasion and progression by various mechanism, it degrades the ECM macromolecules such as collagens, laminins, and proteoglycans which act as a physical barrier to the tumor cell invasion, second, it can modulate cell adhesion, i.e., it helps in the formation of new cell-matrix and cell-cell attachments while breaking the previous (Joyce and Pollard, 2009). MMPs can also enhance angiogenesis by releasing active growth factors and angiogenic factors from the cell surface as well as from the ECM (Suzuki et al., 1997). In the tumor microenvironment, TAM (tumor-associated macrophages), also secrets MMP-9, which cleaves VEGF and sequestered from the matrix, that stimulates new vessel growth, motility, and permeability (Deryugina and Quigley, 2015). It has been reported that MMP-9 knockout mice have collapsed morphology in vessels and diminished metastasis (Deryugina and Quigley, 2015). Similarly, altering the ratio of MMP-2 to TIMP-2 leads to a significant variation in the adhesive phenotype of tumor cells (Stamenkovic, 2000). Therefore, MMPs can also be a good target for the prevention of tumor metastasis and angiogenesis.

During the metastasis, malignant cell detaches from the primary tumor, invade through stromal tissue, enter into the circulation, seized at the peripheral vascular bed, extravasate, and colonized into the target organ (Westermarck and Kähäri, 1999). The initiation of angiogenesis played a very indispensable role in tumor progression and is called an "angiogenic switch," which denotes a shift of dormant cancer to a progressive one (Hanahan and Folkman, 1996, Hanahan and Weinberg, 2011). Tumor-induced angiogenesis is essential for the growth of the primary tumor as well as for the metastases. Without proper vasculature, a tumor cannot grow beyond 23mm size, and therefore, cancer cells often secret certain angiogenic factors to encourage new vasculature formation. The process of tumor-associated sprouting of neovessels from existing blood vessels is referred as a 'tumor angiogenesis' (Folkman, 1971). As the tumor grows in size, the inner mass of the cells, will get less oxygen, and become hypoxic, this hypoxia is known to regulate many 'angiogenic growth factors' in tumor cells (Jain, 2014). These angiogenic factors attract the endothelial cell toward the tumor mass, and these endothelial cells start migrating toward the stimuli and the cells behind, start proliferating and align themselves in the form of a lumen of the newly formed vessel to which blood flow (Bielenberg and Zetter, 2015). These new blood vessels not only provide nourishment to the tumor cells but also act as a site from which the tumor cell enters into the circulation. However, these new tumor vasculatures are not

appropriate; instead, they are tortuous, misguided, malformed, and hyperplastic (Nagy et al., 2010). Among all known angiogenic factors secreted by the malignant tumor cells, perhaps VEGF is the most studied as it plays a significant role in neovascularization. However, the high expression of VEGF in the tumor microenvironment leads to a highly permeable and leaky blood vessel formation. There are many reports of using anti-angiogenic factor in cancer treatment one such example includes Avastin, a VEGF neutralizing antibody termed Bevacizumab has been approved to be used in non-squamous non-small cell lung cancer and colorectal cancer (Carmeliet and Jain, 2011). Therefore, an anti-angiogenic treatment is critical for minimizing the tumor load on the primary organ as well as their metastasis to the distant organ.

There are certain cytokines, and chemokines also reported to be involved in tumor initiation as well as metastasis in A549 cell line, IL-8 is one of them which shows a close association with EMT (Palena et al., 2012), angiogenesis (Koch et al., 1992) cancer cell invasion and metastasis (Bhusari and Khairnar et al., 2014). Other cytokine includes IL-10 which has immunosuppressive property and when express in tumor cell suppress the production of pro-inflammatory cytokines such as TNF-α, IL-6, and IL-1β, thereby metastasis and angiogenesis (Changkija and Konwar, 2012). The IL-6 is known as pro-carcinogenic, and in most of the lung cancer cases, it remains upregulated to assist survival, proliferation, invasion, metastasis, and EMT (Drygin et al., 2011). Most of the non-small cell lung cancer cells also secrete TNF-α and IL-1β, which promotes EMT, invasion, and metastasis (Shang et al., 2017) and they act on cancer cells by establishing a crosstalk with autocrine factors like MMPs, VEGF-α, IL-8, IL-6, and TNF-α hence, facilitate invasion and angiogenesis (Voronov et al., 2003).

In the light of the above review of literature, it is amply clear that a chemotherapic agent which is both cytostatic as well as anti-metastatic, can of immense help in mitigating non-small cell lung cancer which proliferates and invades at a rapid pace resulting in more casualty than usual. Therefore, it was thought pertinent to evaluate the possible anti-metastatic and anti-angiogenic property of 4-fluorophenylacetamide-acetyl coumarin, which was earlier found effective in curtailing proliferation, in the A549 human lung cancer cell line.

MATERIAL AND METHOD

Dose and Duration

The cell line was treated with 0.16nM concentration of 4-FPAC for 48h, as the derivative was found most effective at this concentration and duration of treatment. A stock solution of the

coumarin derivatives was prepared in Dimethylformamide (DMF) or Dimethyl sulfoxide (DMSO). Various dilutions of the derivative were prepared in phosphate buffer saline (PBS), wherein the final concentration of DMF/DMSO was not more than 0.5% in any of the chosen aliquots. The Control group was replaced with vehicle control since there was no significant difference observed between them in terms of parameters studied so far.

A part of this study was carried out using freshly laid eggs of domestic hen (*Gallus domesticus*) of RIR variety. Eggs were procured from the intensive poultry unit of government poultry farm (Vadodara). All the eggs were wiped with 5% w/v povidone-iodine solution and were incubated at 37.5±0.5°C and 75±5% relative humidity post-treatment. Treatment varied group-wise. Eggs were divided into control, vehicle control, and treatment groups. At day 3 of incubation (HH18), 50µl of 4-FPAC was injected, at a concentration of 0.16nM, into the air cell of eggs of treated groups, and the same volume of PBS was injected in the vehicle control group however the control group eggs were kept untreated. All groups were incubated for 48h post-treatment. The *in-ovo* study was conducted in compliance with the protocol approved by an Institutional Animal Ethics Committee (MSU-Z/IAEC/13-2017).

Clonogenic inhibition assay

The clonogenic ability of the cell line under the influence of 4-FPAC was determined by clonogenic inhibition assay. Cells were trypsinized at the log phase, and $1x10^3$ cells/ml were plated on 35mm plate, followed by treatment with 0.16nM of the derivative. After 48h, old media was replaced with a new one, and the cells were further incubated for ten days. After that, cells were fixed and stained with 0.1% crystal violet solution. The number of the colony was counted using a plugin in Fiji (ImageJ, ver 2.0, USA). The surviving fraction can be calculated using the formula:

$$\text{Surviving fraction} = \frac{\text{No of colonies formed after treatment}}{\text{No of cells plated x plating efficiency}}$$

Soft agar assay

Anchorage-independent growth is a decisive property of cancer metastasis and growth. The adhesion-independent growth, under the influence of 4-FPAC, was evaluated, using soft agar assay. 0.8% agarose in FBS free media was used to coat a 35mm disc, once it gets solidified, it was overlaid with 0.4% agarose containing cells and left to solidify. Media with 0.16nM of 4-FPAC was added and incubated for 48h. Then derivative containing media was replaced with a

fresh one and incubated for 10days. On the eleventh day, cells were stained with 0.01% crystal violet solution and photographed under the microscope. The number and size (pixels) of the colony were counted using the plugin in Fiji (ImageJ, ver 2.0, USA).

Wound healing assay

A wound-healing assay was used to analyze cancer cell migration. Cells were seeded on the six-well plate with a density of $2x10^5$ cells/well in media supplemented with 10% FBS. Cells were incubated overnight to adhere and form a monolayer. Once the monolayer reached 90% confluence, it was serum starve overnight, then scratched with the help of a 20µl pipette tip, washed with PBS, and replaced with fresh media containing 0.16nM of 4-FPAC and incubated for 48h. The image was taken at 0h, and 48h using Lawrence and Mayo inverted microscope and evaluated using the plugin in Fiji (ImageJ, ver 2.0, USA). Wound area covering was compared using student's t-test at 95% significance, wherein the experiment was done in triplicates with three scratches each for both control and treated.

Hanging drop aggregation assay

Hanging drop aggregation assay was used to analyze the aggregation property of the A549 cell line. From the stock, $2x10^6$ cells were suspended in 1ml media, containing 0.16nM of 4-FPAC, and for control, the same number of cells were incubated in media without derivative. 30µl of cell suspended media was placed as a droplet on the inner side of the 60mm petri dish lid, and 20 droplets per lid were placed and incubated for 48h. 5ml of media was poured in the disc to avoid drying of droplets. The image was taken at 0h and 48h for both the control and treatment groups. The total area covered by aggregate was analyzed using the plugin in Fiji (ImageJ, ver 2.0, USA), and the mean area of aggregate was expressed in pixels.

Chick chorioallantoic membrane (HET-CAM) test

The anti-angiogenic property of 4-FPAC was analyzed using Hen's Egg Test – Chorioallantoic Membrane (HET-CAM) test. The assay was performed by exposing eggs to various treatments via air sac rather than locally at CAM (Blankenship et al., 2003). At day 3 of incubation, the 50µl of 4-FPAC were added at a concentration of 0.16nM in the eggs of treated groups, the same volume of PBS was added to the vehicle control group, and other eggs were kept untreated. The eggs were incubated for the two days (48h) and rotated on an hourly basis during this period. The embryos were isolated at HH27 (day 5) in the Petri dishes of identical sizes. The CAMs of all eggs were observed under a light microscope (Magnus EM-210, India) and photographed

using catcam eyepiece camera and catymage software (Catalyst Biotech, India). The microvessel density was calculated from the images using the vessel analysis plugin in Fiji (ImageJ, ver 2.0, USA). Statistical analysis of significant differences between means of vessel densities of various groups of eggs was carried out in GraphPad PRISM 5 software using a student's t-test (GraphPad Software Inc., USA).

Quantitative real-time PCR

Total RNA was isolated from the control and treated cells (0.16nM of 4-FPAC for 48h), using TRIzol reagent, and purity of RNA was checked. 1µg of DNAase free RNA was reverse transcribed into cDNA using cDNA Synthesis Kit (Applied Biosystems, USA). Real-time RT-PCR (LightCycler 96 Roche Diagnostics, Switzerland) was performed using primers for genes: *HIF-1α, IL-8, IL-1β TGF- β, IL-10, MMP9, MMP2, TIMP2, TIMP4, E-cadherin, N-cadherin, vimentin, snail1, snail2, ZEB1, claudin 3(CLDN3), claudin 4(CLDN4), VEGF-α, and VEGF-R/KDR* (Primer sequence is provided in Appendix 1). *18sr*RNA was used as an endogenous control for normalization of data. Gel electrophoresis and melt curve analysis were used for confirmation of specific product formation. The Livak method ($2^{-\Delta\Delta Cq}$) was used for calculating the fold change (Livak and Schmittgen, 2001).

Gelatin zymography

$1x10^6$ cells/well were seeded in a six-well plate and incubated overnight, followed by treatment with 0.16nM of 4-FPAC. After 48h, the media was removed, and cells were washed with cold PBS. Thereafter, the cells were homogenized in lysis buffer, centrifuged, and the supernatant was taken. The concentration of protein was estimated using Bradford reagent. 30µg of protein was used for SDS-polyacrylamide gel electrophoresis, containing 2.5% gelatin in resolving gel. Electrophoresis was done at 100V. The gel was washed twice with a Triton wash buffer followed by washes with incubation buffer. It was then incubated overnight at 37°C, followed by staining with 0.25% Coomassie Brilliant Blue for 4h and de-stained till a clear band was seen on blue background.

Western blot analysis

Protein from treated and control cells was harvested, as mentioned for zymography. 40µg of protein was used for the SDS-PAGE electrophoresis. The separated sample was transferred onto the PVDF membrane at 100mA for 20min. After that, blocking was done with TBS containing 0.1% Triton X-100 and 5% skimmed milk for 1h. The membrane was incubated with primary

antibodies which were, monoclonal anti-MMP-9 IgG goat 0.1µg/ml (Sigma Aldrich USA), anti-IL-1β IgG rabbit 0.1µg/ml (Sigma Aldrich USA), anti-VEGF-α IgG goat 0.5µg/ml (DSHB, Iowa), anti-TNF-α IgG mouse 0.1µg/ml (Sigma Aldrich, USA), anti-IL-6 IgG mouse 0.5µg/ml (DSHB Iowa), anti-E-cadherin IgG mouse 0.5µg/ml (DSHB Iowa), anti-N-cadherin IgG mouse 0.5µg/ml (DSHB Iowa), anti-vimentin IgG mouse 0.5µg/ml (DSHB Iowa), and anti-β-actin IgG mouse 0.1µg/ml (Santa Cruz Biotechnology, USA) at $4°C$ for 16h. Followed by three washes with wash buffer, each wash last for 15min and then incubated with corresponding biotinylated secondary antibody (0.5µg/ml) for 45min at room temperature. After that, the membrane was incubated with ALP conjugated streptavidin (0.5µg/ml) for 45min, washed thrice, as mentioned earlier. Bands were developed upon the addition of the BCIP-NBT substrate. Once the specific band was developed, the excess of the substrate was discarded to avoid any nonspecific band development

STATISTICAL ANALYSIS

All values are reported as Mean ± Standard Error of Mean (SEM). The GraphPad PRISM 5 software (GraphPad Software Inc., USA) was used for Statistical analysis. The difference between groups was analyzed using one-way ANOVA followed by Tukey's multiple comparisons test or by Student's t-test. The level of significance was kept at 95%.

RESULT

4-FPAC reduces the clonogenic potential and anchorage-independent growth in A549 cell line

With the onset of ECM remodeling, tumor cells change their typical phenotype to aid metastasis; they lose their anchorage dependency, cell-cell interaction, and establishes a rapid proliferation. These properties of cancer cells were evaluated using soft agar, and clonogenic assay. Soft agar assay was performed for optimizing the anchorage-independent growth of the cancer cells. The result showed that control cells (Figure 3.1C) had proliferated at an average rate on the agar layer and formed a more massive colony. However, cells treated (Figure 3.1D) with 4-FPAC, when observed after 48h of incubation, showed an apparent reduction in the size of the colony (Figure 3.1F, Table 3.2). Nonetheless, no significant difference was observed in the number of colonies as compared to control (Figure 3.1G, Table 3.2.1).

This outcome was reaffirmed with the clonogenic assay (Figure 3.1A, 3.1B), which signifies the colony-forming and proliferation capacity of the cell and found that the derivative treated cells showed reduced clonogenic percentage (Table 3.1), this confirmed that 4-FPAC is negatively affecting the clonogenic property of the A549 cells (Figure 3.1E). Therefore, from both the experiments, it was confirmed that 4-FPAC reduces the anchorage-independent growth and proliferation of the human lung cancer cell line.

4-FPAC increases the cell aggregation property

To initiate metastasis, the cell loses its connections with the neighboring cells as well as with the extracellular matrix and starts moving apart. The effect of 4-FPAC on the aggregation property of cells was determined by hanging drop assay and observed that there was a significant increase in the aggregate size of A549 cells treated with 0.16nM of the derivative compared to the control group (Figure 3.2C). The average size of cell aggregate in case of the control group was 60601 pixels (Figure 3.2A, Table 3.3), nonetheless, when treated with derivative, the mean size of aggregate was increased to 237339 pixels (Figure 3.2A, Table 3.3), which showed that 4-FPAC increases the aggregation property of the selected cancer cell and minimizes the metastasis property of A549 human lung cancer cell line.

4-FPAC reduces the degradation of the extracellular matrix in the A549 cell line

Metastasis initiates with the remodeling of ECM components and is followed by migration to the distant niche. This remodeling is mostly governed by matrix metalloproteinases (MMPs), which degrade type-VI collagen, the main component of ECM (Yang et al., 2009). Here, we observed the effect of 4-FPAC at the selected dose on MMP-9 and MMP-2, the critical players of invasion and metastasis of cancer. At the transcript level, there observed a significant decrease in the expression of *MMP9* and *MMP2* in the treatment group as compared to the control group (Figure 3.3C, Table 3.6). A similar decreasing trend in the MMP-9 was noticed at protein (Figure 3.3A, Table 3.7) and activity level (Figure 3.3B, Table 3.8), hence reaffirming the inhibitory role of 4-FPAC on matrix remodeling. Moreover, there was an upregulation in the expression of *TIMP2* and *TIMP4*, which was noticed in the 4-FPAC treated cells (Figure 3.3C, Table 3.6). This increase in the expression of the negative regulators of MMPs could be a reason behind the observed downregulation of MMPs and thereby, minimizing the ECM degradation in the presence of 4-FPAC.

4-FPAC reduces the expression of EMT regulating genes and transcription factors

During the process of NSCLC progression, EMT is marked as the initiation of cancer metastasis. It is initiated with the disappearance of the basic structures of the epithelia and appearance of mesenchyme characteristics. At the molecular level, we checked the expression of E-cadherin, N-cadherin, and vimentin at mRNA and protein levels. At the transcript level, a significant decrease in *N-cadherin* and an increase in *vimentin*, as well as *E-cadherin*, was observed as compared to their respective controls (Figure 3.4A, Table 3.6). Whereas at the protein level, there was a subtle increase in the expression of E-cadherin and a decrease in vimentin with no significant change in N-cadherin was observed (Figure 3.4D, Table 3.7). Which, further illustrated that the 4-FPAC at the selected dose resists the morphological changes associated with EMT in A549 cells by maintaining the epithelial characteristics by increasing the levels of E-cadherin. It also minimizes the mesenchymal property of the cells by reducing vimentin. Downregulation of *claudin 3*, *claudin 4*, as well as transcription factors namely *Snail1, Snail2,* and *ZEB1,* was also observed in the treated cells (Figure 3.4C, Table 3.6), these transcription factors are known repressors of E-cadherin and facilitate cell migration (Peinado et al., 2007).

4-FPAC reduces cell migration in the A549 cell line

Cancer cell migration plays a decisive role in establishing metastasis and is a frequently used feature to evaluate the anticancer property of any novel derivative. The effect of 4-FPAC on the migration ability of the A549 human lung cancer cell line was estimated by *in vitro* wound closure assay. The result showed a significant reduction in percentage wound coverage in the treated group compared to the control group after 48h of treatment (Figure 3.5A). In treated disc wound cover was 58.42±4.91%, whereas, at the same time, the wound cover percentage in control was 95.0±3.05% (Figure 3.5B, Table 3.4), which confirmed that 4-FPAC reduces the cell migration to exerts its anti-metastatic effect in A549 cell line.

Chick chorioallantoic membrane test

The chick embryo chorioallantoic membrane (HET-CAM) test was carried out to identify the effect of the derivative on the neovascularization process, and it is a very well-established method used in the study of tumor-associated angiogenesis and anti-angiogenesis (Ribatti and Crivellato, 2001, Do Prado et al., 2019). The assay results demonstrated that 4-FPAC is highly anti-angiogenic (Figure 3.6, Table 3.5), which showed a visible difference between control (Figure 3.6A) and treated group (Figure 3.6C), blood vessel densities in one observation field of CAM. The percentage of vessel density in the treated group was 13.3±1.45, on the other hand, in the control group, the percentage of vessel density was 53.04±4.51, which is much higher than

the treated group (Figure 3.6C). The vehicle control group (Figure 3.6B) (56.45±4.08%) did not show any significant variation in the vascularization process compared to the control group proving that the observed reduction in angiogenesis is solely due to 4-FPAC.

4-FPAC reduces the expression of angiogenesis regulating genes and cytokines

Angiogenesis is the critical stage for metastasis, and many putative factors are known to influence it, which includes cytokines, chemokines, and growth factors. Herein, we analyzed the transcript level expression of these factors and found that in 4-FPAC treated cells; there was a significant increase in *TGF- β, VEGF-α, kdr, and HIF-1α* (Figure 3.4A, B). However, a significant decrease was observed in the mRNA level of *IL-8, IL-1β* and *IL-6* in the A549 cells subjected to 0.16nM of 4-FPAC (Figure 3.4B, Table 3.6). Further, no significant change was noted in the level of IL-10 in A549 cells exposed to 4-FPAC (Figure 3.4B, Table 3.6). At the protein level, TNF-α (2.64±0.52) was found to be upregulated whereas, IL-1β and IL-6 were downregulated, and no significant change was observed in the expression of VEGF-α as compared to that of respective controls (Figure 3.4D, Table 3.6).

DISCUSSION

After screening, an array of coumarin derivatives, a C-4 substituted, 4-fluorophenylacetamide-acetyl coumarin derivative was selected. It showed the lowest IC_{50} concentration of 0.16nM with a negligible cytotoxic effect on non-cancerous mouse fibroblast cell line at that concentration. In the previous chapter, we uncovered the mechanism of cell death and observed that the derivative 4-FPAC exerts its cytotoxic effect via ROS mediated and p53 dependent pathway of apoptosis. Parallelly, it was observed that the compound, at a concentration of 0.16nM, has cytostatic property and arrested the A549 cells at the G0/G1 phase of the cell cycle via p53 dependent p21 mediated downregulation of checkpoint regulators namely CDK4/CDK2 cyclins. Since, in most of cancer, the mortality is due to metastatic tumor rather than the primary tumor mass, a chemotherapeutic agent that acts against the mechanism of metastasis, therefore, can evolve as a good drug for future treatment. Nonetheless, in lung cancer, the mortality due to primary tumor is comparable to the metastatic one, therefore, a chemotherapeutic agent that exerts its effect equally on primary tumor along with its metastasis can be of a better cure for this fatal cancer.

In this chapter, the efficacy of 4-FPAC was tested for its potent anti-metastatic property on the A549 human lung cancer cell line. Metastasis is a complex process that involves multiple steps,

including rapid proliferation, EMT, invasion, cell migration, and angiogenesis. Therefore, each of the steps was evaluated using Hanging drop, Clonogenic, Soft agar, Wound closure, and HET-CAM assay.

The cell-cell interaction among the A549 cell line in the presence of the 4-FPAC was analyzed using the hanging drop assay. It is a gravity-driven assay that allows the formation of '3D spheroid,' similar to a microtissue (Timmins and Nielsen, 2007). During the spheroid formation at the base of hanging drop, each cell interacts with others via cell surface molecules such as β1 integrin and cadherin to make cell-cell or cell-ECM interactions. Then, a compact 3D spheroid is produced by cellular contraction of the matrix (Sodek et al., 2009). When A549 cells were treated with 0.16nM of 4-FPAC, a significant increase in the size of tumor spheroid was observed (237339 pixels) than the control group (60601 pixels) that showed that the derivative inhibits metastasis property of A549 cell line by increasing the cell aggregation property of the cells.

When 4-FPAC treated cells were allowed to grow on a disc in the clonogenic assay, a reduction in the colony-forming ability of cells was observed at 48h post-incubation, which shows that the derivative is suppressing the proliferation capability of the A549 cells. The other parameter of metastasis capability includes anchorage-independent growth. The loss of anchorage dependency is the hallmark of the metastatic tumor. Soft agar colony formation assay is the most established method for the characterization of the growth of transformed cells independent of the solid surface *in vitro* and is considered to be one of the stringent tests for the malignant transformation in cells. In this method, cells are prevented from adhering to the culture plate using agar, therefore only transformed cells that do not require a solid substratum to divide can proliferate and form a visible colony (Borowicz et al., 2014). In 4-FPAC treated cells, a significant reduction in the size of the colony was observed on soft agar, which shows that the derivative is not only suppressing the tumor growth as noticed in the clonogenic assay but also affecting the tumor-forming and metastatic potential of the cancer cells.

The migration of the tumor cell is an important step in the cancer cell metastasis, the cell loses its connections, degrades the ECM, and attain the mesenchymal characteristics to migrate and settle in a new niche. A derivative that can prevent the migration of the tumor cells can stop the whole process of metastasis. Therefore, the wound closure assay was performed to check the effect of 4-FPAC on the migration capability of cells, and results revealed that 4-FPAC minimizes the migration of cells about 58.42% compared to that of non-treated one, after 48h post-incubation.

The angiogenesis is the most critical step in tumor proliferation, as well as in metastasis. It supports tumor growth by providing nourishment and acts as an entry site for the metastasized tumor cell. Herein, for the evaluation of the derivative's effect on the angiogenesis, the HET-CAM assay was performed. HET-CAM assay is the extensively used *in vivo* assay in the field of angiogenesis research, in which the highly vascularized chorioallantoic membrane of a chicken embryo is used to analyze the effect of the drug on the growth and development of blood vessels (Hazel, 2003). In the egg, the development of CAM starts from day 3 of incubation (stage 18 of Hamburger and Hamilton) (Hamburger and Hamilton, 1951), therefore, eggs were treated with the 0.16nM concentration of the 4-FPAC at this stage. At day 5 (48h of post-treatment), the effect of derivative on the vascularization process was analyzed, and the result showed a marked decrease in the percentage vessel density in treated CAM (13%) compared to the control one (53%). The above finding is sufficient to deduce that 4-FPAC reduces the angiogenesis required for the metastasis of the A549 cell line.

To understand the molecular events behind these phenomena, specific markers of the pathway that facilitate various processes of metastasis, as mentioned above, were studied in 4-FPAC treated A549 cells at the transcript and protein levels. During metastasis of cancer cell, downregulation of E-cadherin, an epithelial cell surface adhesion molecule, upregulation of N-cadherin, a mesenchymal cell surface adhesion molecule and Vimentin, an intermediate filament protein were observed. All these are usually associated with epithelial to mesenchymal transition (EMT), which helps cancer cells to migrate from one niche to another (Wheelock et al., 2008). Therefore, the transcription regulators of EMT, namely Snail1, Snail2, and ZEB1, were analyzed. Results revealed a significant reduction in the expression of *Snail1, Snail2, and ZEB1* in the A549 cells treated with 4-FPAC. The Snails and ZEB1 are known to induce EMT by downregulating the cell adhesion molecules and upregulating intermediate filaments that facilitate cell migration (Savagner, 2001; Jiang et al., 2011). Besides, reduction in the levels of adhesion molecules like *claudin 3* and *claudin 4* was also observed in the treated cells, which could be a function of Snail mediated expression of a transcriptional inhibitor named ZEB1. Similar observations by Lin and co-workers (2013) give credence to the present result (Lin et al., 2013). Moreover, it has been reported that when p53 expression increases, it degrades Snail2 via MDM2 interaction (Wang et al., 2009). Therefore, it is prudent to presume that the observed hike in p53 expression (as detailed in Chapter 2) might be the reason behind the reduction in *snail* 2 levels in the treated cells. Furthermore, the compromised expression of *snail 2,* in turn*,* influences the expression of *ZEB1*, a downstream modulator of the Snail pathway, resulting in a

substantial reduction of EMT in A549 cells challenged with 4-FPAC. Additionally, the reduced expression of PCNA (as mentioned in Chapter 2), a proliferation marker, further substantiates the reduction in clonogenic capacity exhibited by A549 cells exposed to 4-FPAC. Therefore, it could be inferred that 4-FPAC affects the EMT initiation process by upregulating E-cadherin via Snail activated downregulation of ZEB1 in A549 cells.

However, once EMT has initiated, the process will be maintained by the autocrine loop of growth factors like TGF-β (Xu et al., 2009). The TGF-β chiefly support EMT by activating transcription factors like Twist, Snail1, and ZEB1, which downregulates E-cadherin and upregulates Vimentin and N-cadherin (Vincent et al., 2009). TGF-β is also known to induce ROS by reducing the levels of antioxidant enzymes like glutathione peroxidase, SOD, and catalase (Liu and Pravia, 2010) similar observation was noticed in the previous chapter (Chapter 2). The rapid proliferating cell shows a condition of hypoxia that is due to the lack of blood supply in the inner mass of cells and secrets, a factor called HIF-1α. The HIF-1α, along with TGF-β, activates the secretion of matrix metalloproteinases (MMPs) under the influence of Snail from the tumor cells undergoing EMT (Ota et al., 2009). The MMPs further degrades the basement membrane, and cells start the migration from one site to another via lymph node. The activated Snail induces IL-8 and VEGF-α, which initiates neovascularization near tumor cells (Du et al., 2008, Hwang et al., 2011). The VEGF-α also activates EMT via HIF-1α mediated Snail pathway in the same way as hypoxia induces the process of neovascularization (Mak et al., 2010).

Therefore, based on the literature, the effect of 4-FPAC on the process of metastasis was analyzed. The result unveiled that 4-FPAC increases the expression of *TGF-β,* which leads to the augmentation of ROS and thereby upregulating *HIF-1α*. Nonetheless, this upregulation was not enough to prevent Snail degradation and release of MMP-2 and MMP-9, as both were found to be decreased in treated cells. At the same time, a decrease in protein level expression of IL-8 was also observed, which might be because of the downregulation of *snail* and MMPs, as reported by Lewis and others (Lewis et al., 2006). This downregulation of IL-8 might be responsible for the anti-angiogenic property of 4-FPAC. Moreover, p53 is known as a negative regulator of VEGF-α promoter activity (Mukhopadhyay et al., 1995), and in the treated cells, there was a significant reduction in the expression of p53. Therefore, it can be inferred that p53 and Snail were the major inhibitors of the metastasis and angiogenesis in the A549 cells treated with 4-FPAC.

Other factors have also been suggested to be involved in the initiation as well as maintenance of metastasis, these are IL-6, IL-10, TNF-α, and IL-1β, which, too, were studied herein to corroborate the earlier described anti-metastatic property of 4-FPAC in A549 cells. IL-10 is reported to be a suppressor of metastasis and angiogenesis (Silvestre et al., 2000). However, in most of the lung cancer cases, IL-6 remained upregulated to assist survival, proliferation, invasion, metastasis, and EMT (Shintani et al., 2016). Most of the non-small cell lung cancer secrete IL-6 and TNF-α, which promotes EMT, invasion, and metastasis (Shang et al., 2017). IL-1β, which is produced by cancer cells itself, acts on cancer cells by establishing a crosstalk with autocrine factors like MMPs, VEGF-α, IL-8, IL-6, and TNF-α hence, facilitate invasion and angiogenesis (Voronov et al., 2003). In this study, a significant elevation in the transcript levels of *IL-10* and a concomitant reduction in the mRNA levels of *IL-6* and *IL-1β* was observed in 4-FPAC treated cells, which reiterate the anti-metastatic potential of the compound in question. Nonetheless, the expression of TNFα was found significantly increased in the cells subjected to 0.16nM of 4-FPAC. However, apart from its reported prometastatic property, TNF-α is also an activator of the Fas-mediated apoptotic pathway, and ROS mediated necrotic pathway (Thorburn, 2004). Hence, this increase in TNF-α could be to assist the extrinsic pathway of apoptosis as described in the previous chapter.

Briefly, 4-FPAC is effective in curtailing the metastasis and angiogenesis in A549 cells by p53 mediated downregulation of TGF-β, Snails, MMP-2, 9, and IL-8. The currently observed anti-tumor and anti-angiogenic efficacy of 4-FPAC on A549 human lung cancer cell line suggest that it has the potential to evolve as a promising novel chemotherapeutic agent against non-small cell lung cancer.

SUMMARY

Among all types of the cancer reported, lung cancer has the highest mortality rate. There are much reasons behind such a high mortality rate. First, it is the preferred niche for the metastasized tumor of any origin, and second, in lung cancer, the primary tumor is as death-defying as the metastasized one (Nguyen et al., 2009). Hence, a chemotherapeutic agent that can limit the tumor at the primary site and combat with each step of metastasis without affecting the normal neighborhood cells can act as a promising medication for future use. In search of such a potential candidate, we screened an array of coumarin derivatives and reached to the 4-fluorophenylacetamide-acetyl coumarin derivative, which showed a negligible side-effect to the non-cancerous cell line NIH3T3 with very minimal concentration *viz.,* 0.16nM. The derivative also induced apoptotic cell death in the A549 cell line through ROS induced DNA damage and p53 mediated caspase-dependent pathway. Further analysis of its anti-metastasis potential and anti-angiogenic potential was evaluated with the help of Hanging Drop, Clonogenic, Soft-Agar, Wound Healing, and HET-CAM assay. The hanging drop and wound healing assay revealed that 4-FPAC minimizes the migration to the distant organ by reducing the cell to cell and cell to matrix connections. The clonogenic and soft-agar assay revealed that 4-FPAC has the potential to combat the growth as well as its tumor-forming potential of the NSCLC cell line. The CAM assay was used to measure the anti-angiogenic property of 4-FPAC and showed a marked decrease in the percentage of vascularization in the chick chorioallantoic membrane at day 5 post-incubation. The molecular-level analysis confirmed that the process of EMT was minimized because of p53 dependent Snail mediated upregulation of E-cadherin and downregulation of N-cadherin. The treatment also reduced ECM remodeling because of downregulation of MMPs due to the influence of TGF-β and Snail. The anti-angiogenic property was due to Snail mediated downregulation of chemokine IL-8. Therefore, the primary mediator behind the anti-metastasis property of the compound is p53 and Snail. Overall, the 4-FPAC has anti-proliferative, anti-metastatic, and anti-angiogenic properties with which it can be used as a future chemotherapeutic for the treatment of NSCLC. The entire work and results are graphically summarized in Figure 3.7.
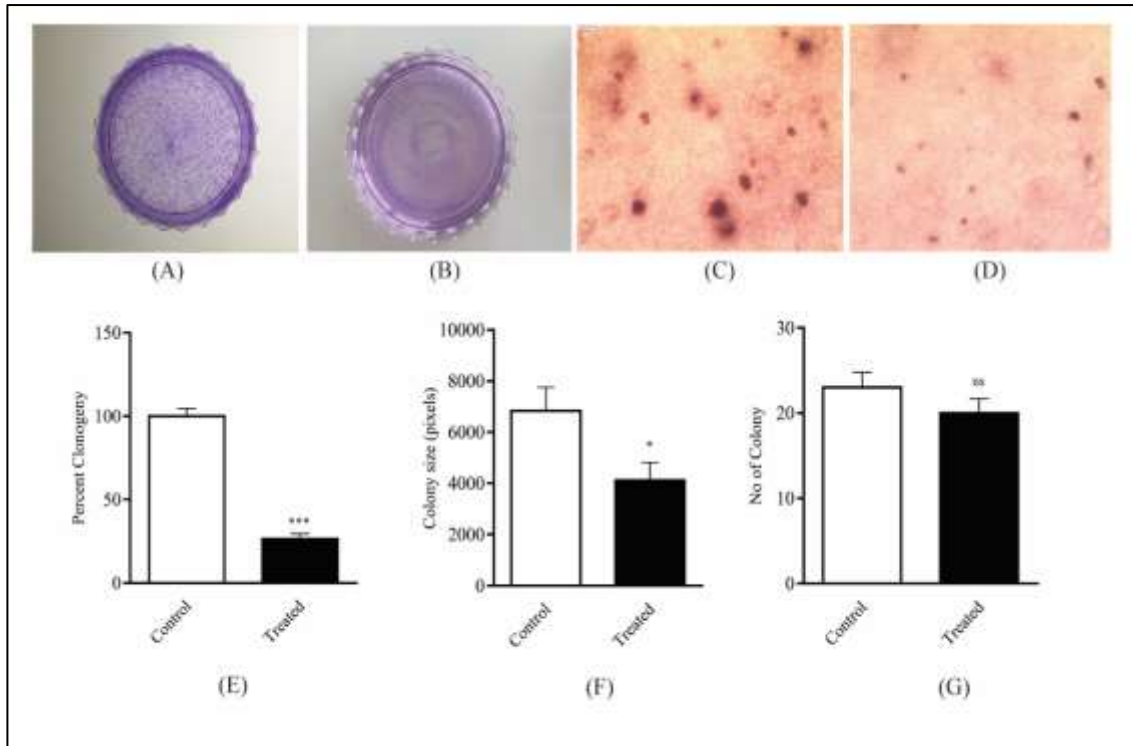
Figure. 3.1. Effect of 4-FPAC on anchorage-independent growth and clonogenic property of A549 cell line: Clonogenic inhibition assay depicting control (A) and treated (B) colonies at 48h post-treatment. (E) The graph represents clonogenic inhibition in treated condition, n=5. Soft agar assay for control (C) and treated (D) cell lines, at 48h post-treatment. Graphs are representing the size of the colony (F) and the number of the colony (G) on agar. Data is represented as Mean ± Standerd Mean of Error (SEM). The comparison for statistical significance is made between control (0nM) and treated (0.16nM) using a student's t-test and denoted as, ***p≤0.001 and *p≤0.05, ns=not significant.
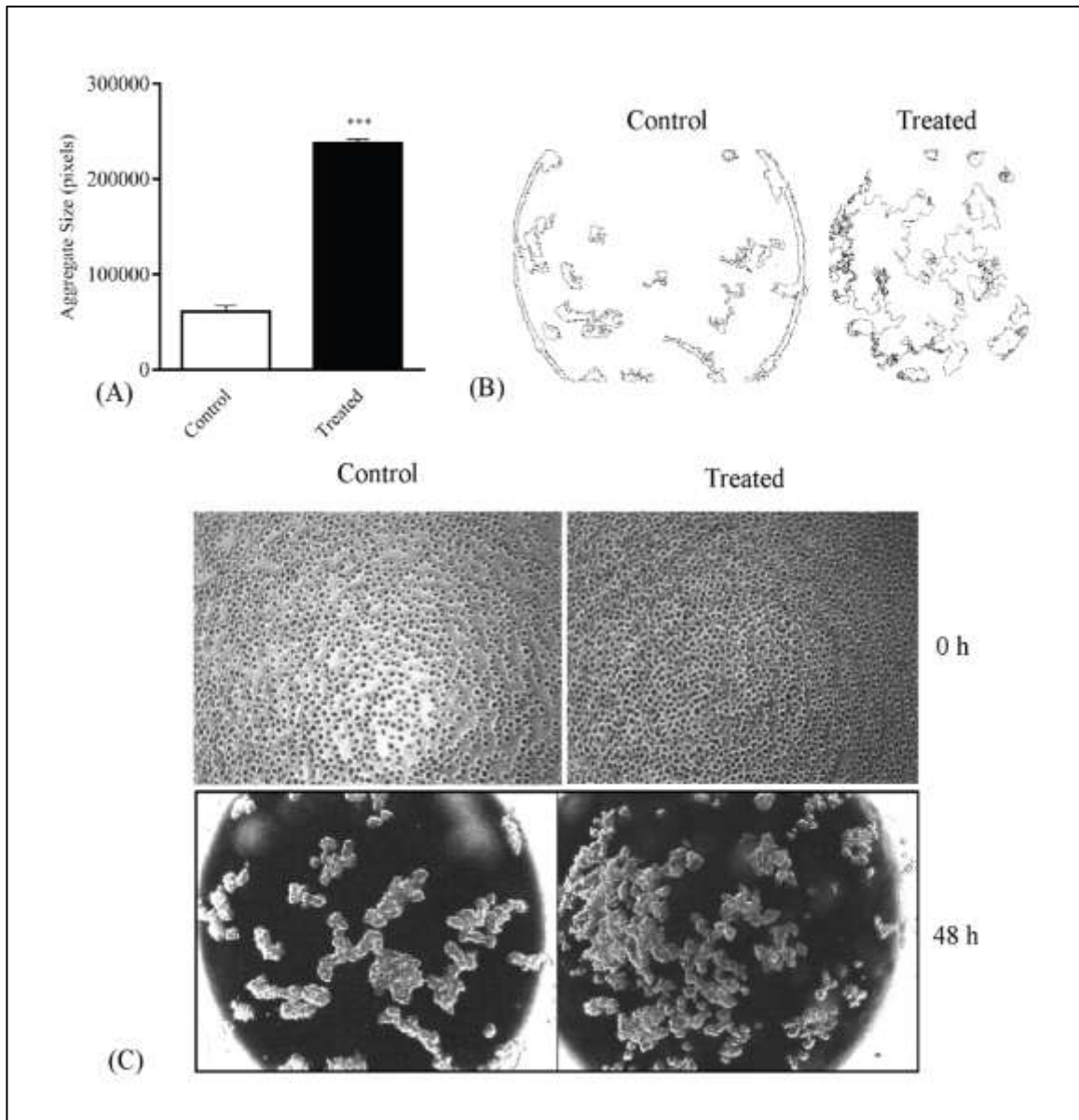
Figure 3.2. Hanging drop assay for the analysis of aggregation property of A549 cell line upon treatment with 4-FPAC; Graph represents the aggregate size (in pixels) (A). Representative Images of aggregate in control (0nM) and treated cell (0.16nM) at 48h (B). Photomicrographs of hanging drop assay for control and treated at 0h and 48h (C). Data is represented as Mean ± Standard Error of Mean (SEM). The comparison for the statistical significance is made between control (48h) and treated (48h). The level of significance is denoted as, ***p≤0.001.
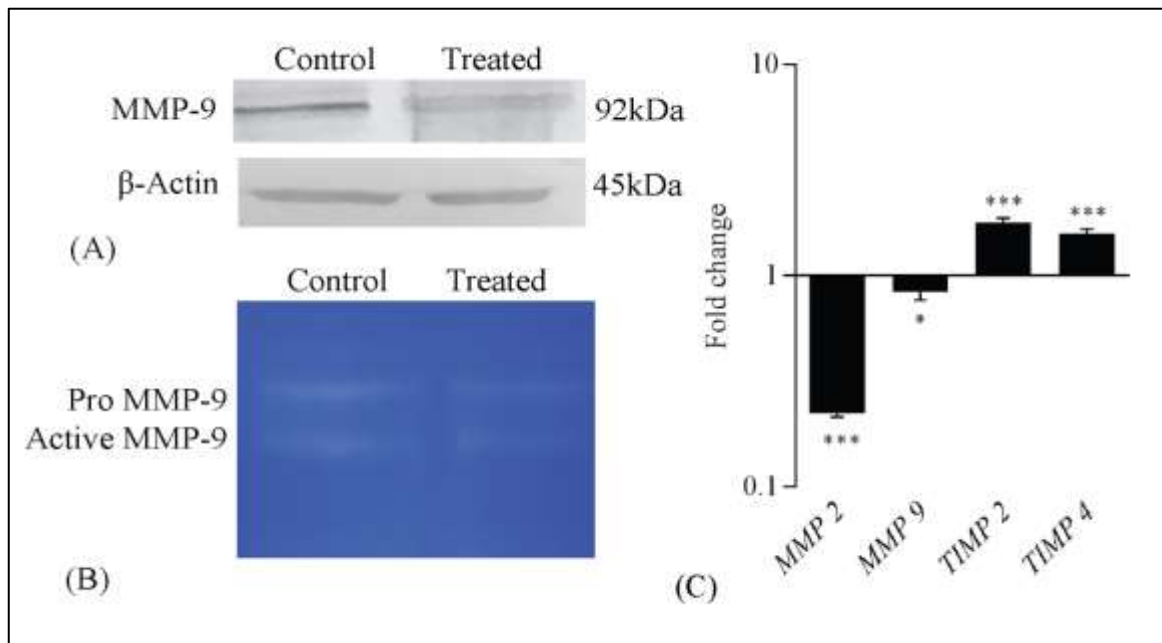
Figure 3.3. Effect of 4-FPAC on ECM Remodeling in A549: (A) Western blot analysis of MMP9 in control (0nM) and treated (0.16nM) group, β-actin was taken as an internal control. (B) Gelatin zymogram for MMP-9 activity. (C) qRT-PCR of genes involved in migration. Values are expressed as Mean ± Standard Error of Mean (SEM). Fold change values for control is 1. ***p≤0.001 and *p≤0.05.
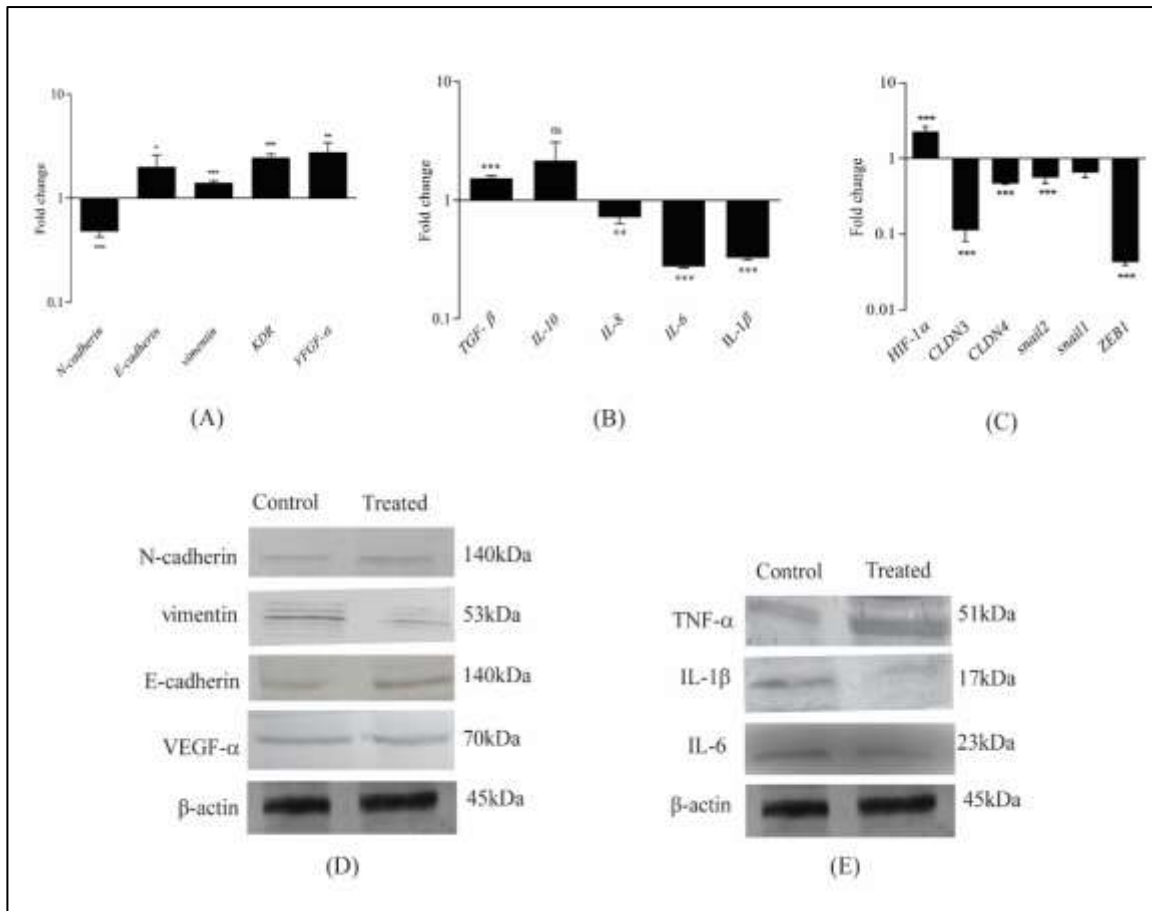
Figure 3.4. Analysis of Metastasis and angiogenesis in A549 cell line: qRT-PCR of genes involved in metastasis and angiogenesis depicted in (A), (B) and (C). Values are expressed as Mean ± Standard Error of Mean (SEM). Fold change values for control is 1. ***p≤0.001, **p≤0.01, and *p≤0.05. (C) (D) and (E) Western blot analysis of key regulators involved in; EMT: E-cadherin, N-cadherin, and vimentin, Angiogenesis: VEGF-α, and cytokines: TNF- α, IL-1β, IL-6, in control and treated group, β-actin was taken as an internal control.
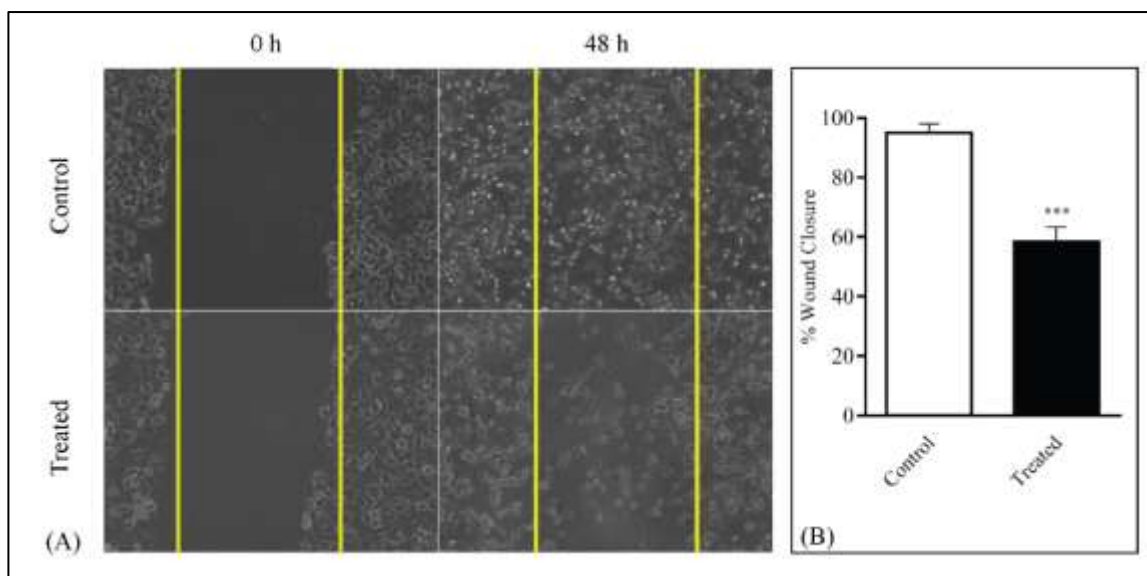
Figure 3.5. Wound closure assay for the analysis of migration property of A549 cell line upon treatment with 4-FPAC: Photomicrograph of control (0nM) and treated (0.16nM) cells at 0h and 48h (A). The graph representing the percentage wound area cover in control and treated cell line (B). Data expressed as Mean ± Standard Error of Mean (SEM). The experiment was performed in triplicate. The comparison for statistical significance is made between control (48h) and Treated (48h) group using student's t-test and denoted as, ***p≤0.001
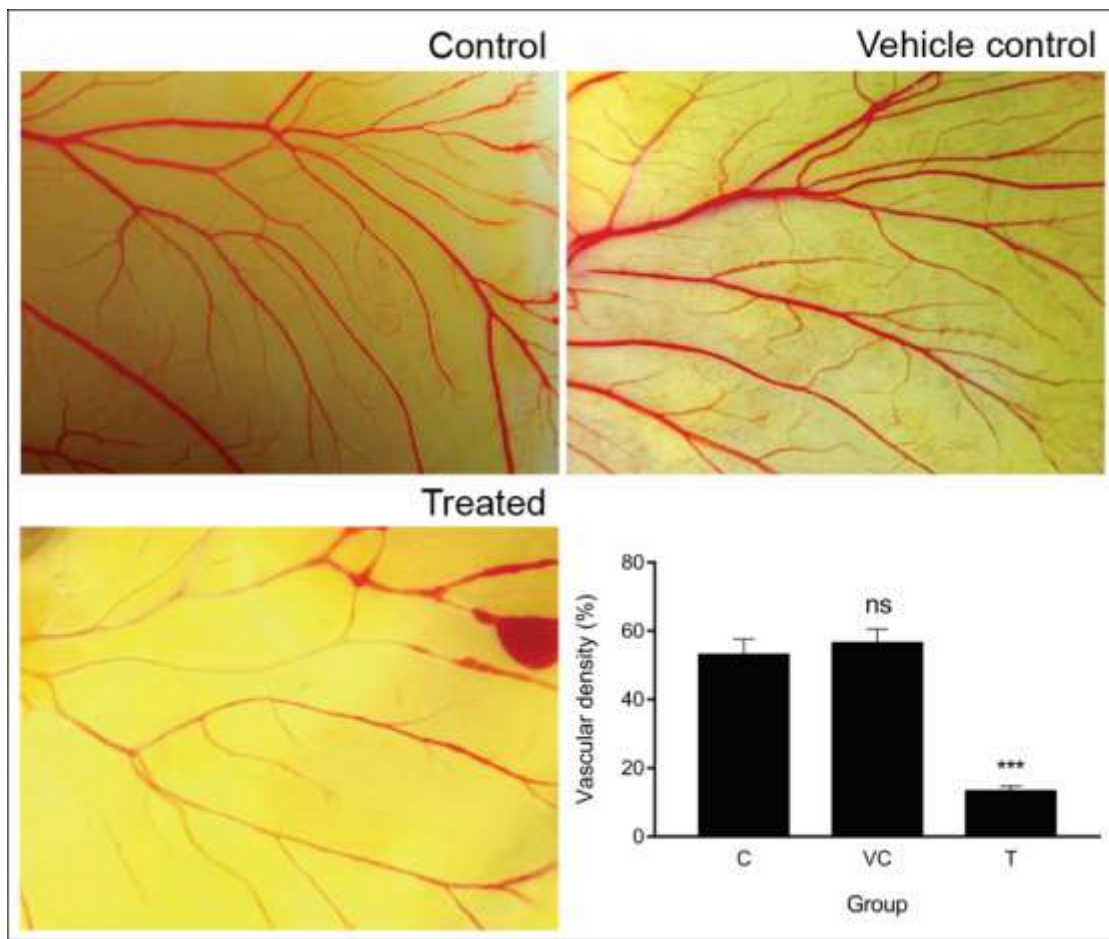
Figure 3.6. Chick chorioallantoic assay (CAM assay) for the analysis of angiogenesis upon treatment with 4-FPAC. The representative image of control (A), vehicle control (B), and 4-FPAC Treated (0.16nM). The graph is representing the percent vascular density in control (C), vehicle control (VC), and Treated (T). Data is representing as Mean ± Standerd Error of Mean (SEM). The comparison for the statistical significance is made control, and denoted as ***P<0.001, ns=not significant.

Groups	Percentage Clonogeny (Mean± SEM)
Control	100 ±10.1
Treated	26.41±7.08***

Table 3.1. Comparative analysis of clonogenic property of control and 4-FPAC treated (0.16nM) A549 cell line. The experiment was performed in triplicate. The comparison for statistical significance is done with the control group (0nM) and denoted as ***p≤0.001.

Groups	Colony size (Pixels)
Control	6836.71± 918.8
Treated	4112.8±710.84*

Table 3.2. Comparative analysis of colony size of control and treated on Soft agar plate; the experiment was performed in triplicate and represented in pixels. The comparison for statistical significance is done between the control (0nM) and treated group (0.16nM) and denoted as *p≤0.05.

Group	Number of colony (Mean±SEM)
Control	23.2±4.0
Treated	20±3.8^{ns}

Table 3.2.1. Comparative analysis of number of the colony on Soft agar plate; the experiment was performed in triplicate. The comparison for statistical significance is done between the control (0nM) and treated (0.16nM) group and denoted as ns=not significant.

Groups	Aggregate Size (Mean±SEM)
Control	60601±37310.5
Treated	237339±15822.6***

Table 3.3. Comparative analysis of aggregate size using Hanging drop assay in A549 cell line; The comparison for statistical significance is done between the control (0nM) and treated (0.16nM) group using student's t-test and denoted as, ***$p \leq 0.001$.

Groups	Percentage Wound closure (Mean±SEM)
Control	95.30±3.05
Treated	58.42±4.9***

Table 3.4. Comparative analysis of percentage wound closure assay in the A549 cell line. The comparison for statistical significance is done between the control (0nM) and treated (0.16nM) group using student's t-test and denoted as ***$p \leq 0.001$.

Groups	Percentage Vessel Density (Mean±SEM)
Control	53.04±4.51
Vehicle Control	56.45±4.086[ns]
Treated	13.3±1.45***

Table 3.5. Comparative analysis of anti-angiogenic property of 4-FPAC using Chick chorioallantoic assay (HET-CAM) in A549 cell line. Data representing the percent vessel density in control, vehicle control, and treated (0.16nM) cell, n=5. The comparison for statistical significance is done with the control group using one way ANOVA, and denoted as ***$p \leq 0.001$, ns=not significant.

Gene	Fold change (Mean± SEM)
MMP9	$0.223 \pm 0.0008^{***}$
MMP2	$0.836 \pm 0.069^{*}$
TIMP2	$1.78 \pm 0.09^{***}$
TIMP4	$1.59 \pm 0.07^{***}$
N-cadherin	$0.48 \pm 0.056^{***}$
E-cadherin	$2.006 \pm 0.6^{*}$
vimentin	$1.409 \pm 0.074^{***}$
VEGF-α	$2.47 \pm 0.19^{***}$
Kdr	$2.77 \pm 0.65^{**}$
HIF-1 α	$2.281527 \pm 0.38^{***}$
CLDN3	$0.113 \pm 0.032^{***}$
CLDN4	$0.466 \pm 0.0076^{***}$
snail2	$0.56 \pm 0.09^{***}$
snail1	$0.65 \pm 0.08^{***}$
ZEB1	$0.043 \pm 0.004^{***}$
TGF-β	$1.53 \pm 0.076^{***}$
IL-10	2.15 ± 0.93^{ns}
IL-8	$0.719 \pm 0.083^{**}$
IL-6	$0.277 \pm 0.008^{***}$
IL-1 β	$0.328 \pm 0.16^{***}$

Table 3.6. qRT-PCR analysis of genes involved in 4-FPAC induced apoptotic death. The fold change value of the control group was 1.0. The level of significance is denoted as***p≤0.001, **p≤0.01.

Protein	Relative Density (Fold change)
TNF-α	$2.64 \pm 0.52^{**}$
IL-1β	$0.87 \pm 0.025^{*}$
IL-6	$0.81 \pm 0.01^{*}$
VEGF-α	0.94 ± 0.06^{ns}
MMP-9	$0.32 \pm 0.001^{***}$
E-cadherin	$1.62 \pm 0.31^{**}$
N-cadherin	0.88 ± 0.061^{ns}
Vimentin	$0.36 \pm 0.08^{**}$

Table 3.7. Quantification of western blots using Plugin Fiji (Image J, ver. 2.0, USA) software represented as Relative Density (fold change) for a major protein involved in metastasis and angiogenesis. The comparison for statistical significance was made for 4-FPAC treated group with the control group. Data is represented as Mean $\pm$ Standerd Error of Mean (SEM), and the level of significance is denoted as, ***$p \leq 0.001$, **$p \leq 0.01$, **$p \leq 0.01$ *$p \leq 0.05$, ns=not significant.

Protein	Relative Density (Mean$\pm$SEM)
MMP-9	$0.78 \pm 0.06^{***}$

Table 3.8. Quantification of MMP-9 activity using Gelatin zymography using Plugin Fiji (Image J, ver. 2.0, USA) software represented by Relative Density (fold change). The comparison for statistical significance was made for 4-FPAC treated group with the control group. Data is represented as Mean $\pm$ Standard Error of Mean (SEM), and the level of significance is denoted as***$p \leq 0.001$.
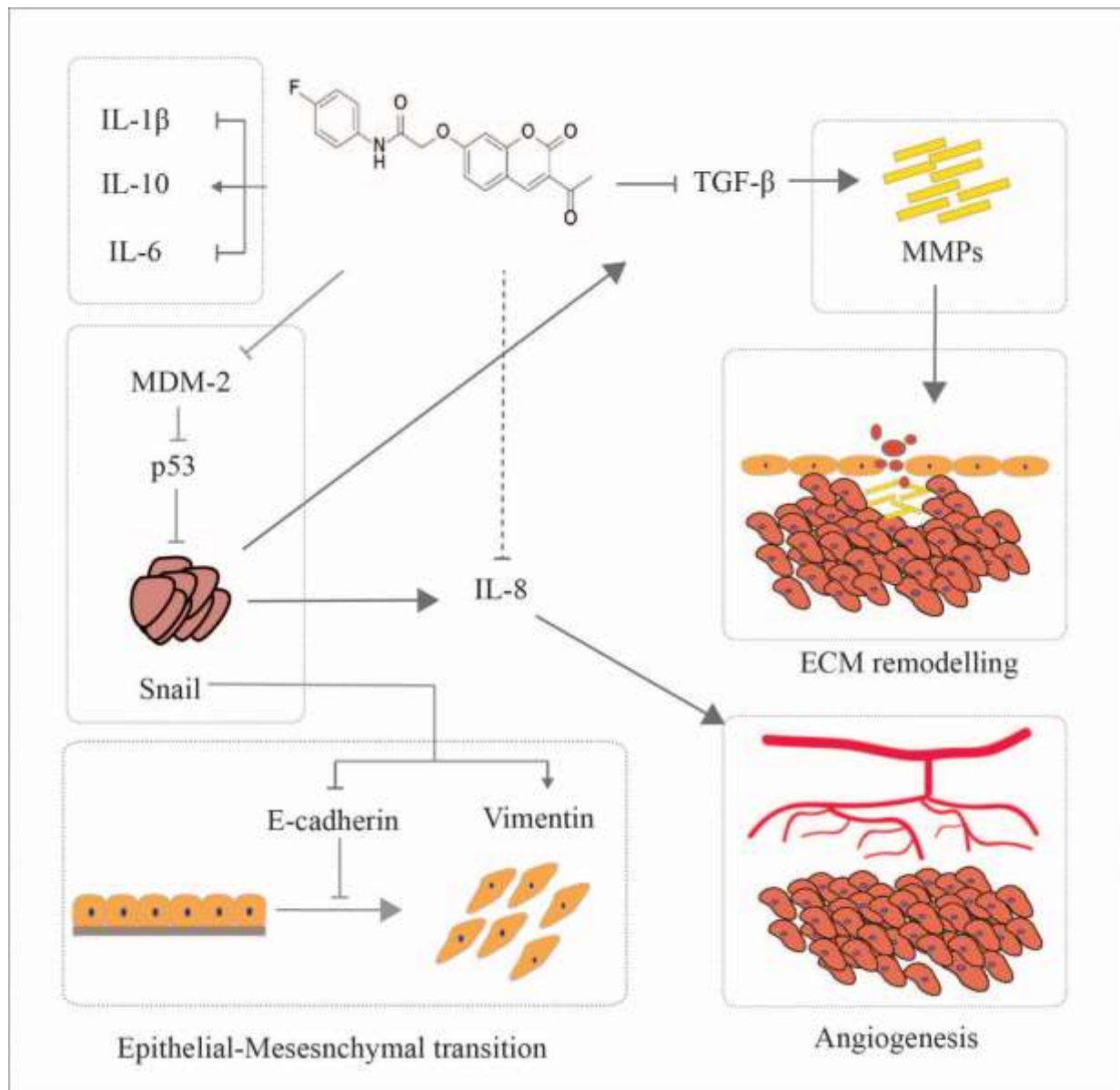
GRAPHICAL SUMMARY

Figure. 3.7. Anti-metastatic and anti-angiogenic activity of 4-FPAC